

Transmitting Important Bits and Sailing High Radio Waves: A Decentralized Cross-Layer Approach to Cooperative Video Transmission

Nicholas Mastronarde, *Member, IEEE*, Francesco Verde, *Member, IEEE*, Donatella Darsena, *Member, IEEE*, Anna Scaglione, *Fellow, IEEE*, and Mihaela van der Schaar, *Fellow, IEEE*

Abstract—We investigate the impact of cooperative relaying on uplink multi-user (MU) wireless video transmissions. We analyze and simplify a MU Markov decision process (MDP), whose objective is to maximize the long-term sum of utilities across the video terminals in a decentralized fashion, by jointly optimizing the packet scheduling and physical layer, under the assumption that some nodes are willing to act as cooperative relays. The resulting MU-MDP is a pricing-based distributed resource allocation algorithm, where the price reflects the expected future congestion in the network. Compared to a non-cooperative setting, we observe that the resource price increases in networks supporting low transmission rates and decreases for high transmission rates. Additionally, cooperation allows users with feeble direct signals to significantly improve their video quality, with a moderate increase in total network energy consumption that is far less than the energy these nodes would require to achieve the same video quality without cooperation.

Index Terms—Cooperative communications, cross-layer optimization, Markov decision process, wireless video transmission.

I. INTRODUCTION

A SUBSTANTIAL body of work is devoted to the cross-layer adaptation of wireless multi-user (MU) video streaming, to match available system resources (e.g., bandwidth, power, or transmission time) to application requirements (e.g., delay or source rate), and vice versa. Cross-layer optimizations proposed in [1]-[3] strike a balance between scheduling lucky users who experience very good fades, and serving users who have the highest priority video data to transmit. This tradeoff is important because rewarding a few lucky participants, as opportunistic multiple access policies do [4]-[5], does not translate to providing good quality to the application (APP) layer. Unfortunately, the aforementioned work assumes that wireless users are *non-cooperative* and,

occasionally, users with higher priority video data, but worse fades, use the wireless channel. A way to not let good fades go to waste is to enlist the nodes that experience good fades as cooperative helpers, using a number of techniques available for cooperative coding [6]-[8] as in [9]-[10]. The work in [10] proposes a cross-layer optimization of the physical (PHY) layer, the medium access control (MAC) sublayer, and the APP layer, for efficient multicasting from a single source. In [9], a centralized network utility maximization (NUM) framework is proposed for jointly optimizing relay strategies and resource allocations in a cooperative orthogonal frequency-division multiple-access network. In both [9], [10], it is assumed that each user has a static utility function of the average transmission rate.

This paper is the first considering the dynamic optimization of MU video streaming in cooperative networks. Unlike [9], [10], the solution that we adopt explicitly considers packet-level video traffic characteristics (instead of flow-level) and dynamic network conditions (instead of average conditions). Specifically, we first formulate the cooperative wireless video transmission problem as an MU-MDP using a time-division multiple-access (TDMA)-like network, randomized space-time block coding (STBC) [11], and a decode-and-forward cooperation strategy. We show analytically that the decision to cooperate can be made opportunistically, independently of the MU-MDP. Consequently, each user can determine its optimal scheduling policy by only keeping track of its experienced cooperative transmission rates, rather than tracking the channel statistics throughout the network. Second, we use this insight to design a *self-selection* strategy to enlist cooperative nodes, that requires the exchange of a number of messages which is linear in the number of video sources. Third, we show experimentally that users with feeble direct signals to the access point (AP) are conservative in their resource usage when cooperation is disabled. In contrast, when cooperation is enabled, users with feeble direct signals to the AP use cooperative relays and utilize resources more aggressively. Fourth, we study the impact of cooperation on the total network energy consumption.

II. SYSTEM MODEL

We consider M users streaming video over a shared wireless channel to a single AP.

Time is slotted into discrete time-intervals of length $R > 0$

Manuscript received 1 February 2011; revised 20 July 2011. The work of M. van der Schaar and N. Mastronarde was supported in part by NSF grant no. 0831549 and of A. Scaglione by NSF grant no. 905267.

N. Mastronarde is with the Department of Electrical Engineering, State University of New York at Buffalo, NY, USA (e-mail: nmastron@buffalo.edu).

F. Verde is with the Department of Biomedical, Electronic and Telecommunication Engineering, University Federico II, Naples, Italy (e-mail: f.verde@unina.it).

D. Darsena is with the Department for Technologies, Parthenope University, Naples, Italy (e-mail: darsena@unina.it).

A. Scaglione is with the Department of Electrical and Computer Engineering, University of California Davis, CA, USA (e-mail: ascaglione@ucdavis.edu).

M. van der Schaar is with the Department of Electrical Engineering, University of California at Los Angeles (UCLA), CA, USA (e-mail: mihaela@ee.ucla.edu).

Digital Object Identifier 10.1109/JSAC.2012.121002.

seconds and each time slot is indexed by $t \in \mathbb{N}$.¹ At the MAC sublayer, the users access using a TDMA schedule: in time slot t , the AP endows the i th user, for $i \in \{1, 2, \dots, M\}$, with the resource fraction x_t^i , where $0 \leq x_t^i \leq 1$, such that the user can use the amount of channel time $R x_t^i$ for transmission. Let $\mathbf{x}_t \triangleq (x_t^1, x_t^2, \dots, x_t^M)^T \in \mathbb{R}^M$ denote the resource allocation vector at time slot t , which must satisfy the stage resource constraint $\|\mathbf{x}_t\|_1 = \sum_{i=1}^M x_t^i \leq 1$, where the inequality accounts for possible signaling overhead.

The PHY layer is assumed to be a single-carrier single-input single-output system, using quadrature amplitude modulation (QAM) square constellations, with a (fixed) symbol rate of $1/T_s$ (symbols/second). The PHY layer can support a set of $N + 1$ data rates $\beta_n \triangleq b_n/T_s$ (bits/second), where $b_n \triangleq \log_2(M_n)$ is the number of bits that are sent every symbol period, with $n \in \{0, 1, \dots, N\}$, and M_n is the number of signals in the QAM constellation. Hence, $\beta_0 \leq \beta_1 \leq \dots \leq \beta_N$ form the *basic rate set* \mathcal{B} and β_0 is the *base rate* at which the nodes exchange control messages. Let d_n be the minimum distance of the M_n -QAM constellation. It is well known that the average transmitter energy per symbol is given by $\mathcal{E}_s \triangleq d_n^2 \left(\frac{M_n-1}{6}\right)$ (Joules), fixed for all the nodes and data rates (the average transmit power per symbol is $\mathcal{P}_s \triangleq \mathcal{E}_s/T_s$ Watts). We consider a frequency flat block fading model, where $h_t^{i\ell} \in \mathbb{C}$ denotes the fading coefficient over the $i \rightarrow \ell$ link in time slot t , with $i \neq \ell \in \{0, 1, \dots, M\}$, and $i = 0$ or $\ell = 0$ corresponding to the AP. It is assumed that all the channels are dual, i.e., $|h_t^{i\ell}| = |h_t^{\ell i}|$, and that $h_t^{i\ell}$ are independent and identically distributed (i.i.d.) with respect to t . Moreover, we define $\mathbf{H}_t \in \mathbb{C}^{M \times M}$ as the matrix of all the fading coefficients, i.e., $\{\mathbf{H}_t\}_{i\ell} = h_t^{i\ell}$, for $i \neq \ell \in \{0, 1, \dots, M\}$.

At the PHY layer, there are two transmission modes. In the *direct* transmission mode, the i th source node transmits directly to the AP at the data rate $\beta_t^{i0} \in \mathcal{B}$ (bits/second) for $R x_t^i$ seconds. In the *cooperative* transmission mode, some nodes serve as decode-and-forward relays. Specifically, in the cooperative mode, the assigned transmission time is divided into two phases: in *Phase I*, the i th source node directly broadcasts its own data to all the nodes in the network at the data rate $\beta_t^{i,1} \in \mathcal{B}$ for $R \rho_t^i x_t^i$ seconds, where $0 < \rho_t^i < 1$ is the Phase I time fraction; in *Phase II*, a subset of the nodes $\mathcal{C}_t^i \subseteq \{1, 2, \dots, M\} - \{i\}$, demodulate the data received in Phase I, re-modulate the original source bits, and then cooperatively transmit towards the AP, along with the original source i , at the data rate $\beta_t^{i,2} \in \mathcal{B}$ for the remaining $R(1 - \rho_t^i) x_t^i$ seconds. In the sequel, $\beta_t^{i,\text{coop}}$ (bits/second) is the *cooperative data rate* over the two phases, i.e., the amount of bits that are transmitted in each phase divided by the total duration of the two phases, which depends on the data rates $\beta_t^{i,1}$ and $\beta_t^{i,2}$

¹Complex, real, and nonnegative integer fields are \mathbb{C} , \mathbb{R} , and \mathbb{N} , respectively; matrices [vectors] are denoted with upper [lower] case boldface letters (e.g., \mathbf{A} or \mathbf{x}); the superscript T denotes the transpose; $|\cdot|$ is the magnitude of a complex number; $\|\mathbf{x}\|_1$ is the l_1 and $\|\mathbf{x}\|_2$ is the Euclidean norm of $\mathbf{x} \in \mathbb{C}^n$; $\{\mathbf{A}\}_{ij}$ indicates the $(i+1, j+1)$ th element of the matrix $\mathbf{A} \in \mathbb{C}^{m \times n}$, with $i \in \{0, 1, \dots, m-1\}$ and $j \in \{0, 1, \dots, n-1\}$; a circular symmetric complex Gaussian random variable X with mean μ and variance σ^2 is denoted as $X \sim \mathcal{CN}(\mu, \sigma^2)$; $\lfloor \cdot \rfloor$ and $\lceil \cdot \rceil$ denote floor- and ceiling-integer, respectively; $E[\cdot]$ stands for ensemble averaging; and $[\cdot]^+ = \max(\cdot, 0)$.

attainable in each of the two hops. The cooperation decision is denoted by $z_t^i \in \{0, 1\}$, where $z_t^i = 1$ if cooperation is chosen, and $z_t^i = 0$ if direct transmission is chosen.

The deployed traffic model, so long as it is Markovian, is not critical to our results. But for concreteness, and in experiments, we follow the model in [3]. For $i \in \{1, 2, \dots, M\}$, the *traffic state* $\mathcal{T}_t^i \triangleq \{\mathcal{F}_t^i, \mathbf{b}_t^i\}$ represents the video data that the i th user can potentially transmit in time slot t , including the schedulable frame set \mathcal{F}_t^i and the buffer state \mathbf{b}_t^i . In time slot t , we assume that the i th user can transmit packets in \mathcal{F}_t^i whose deadlines are within the scheduling time window (STW) $[t, t+W]$. The buffer state $\mathbf{b}_t^i \triangleq (b_{t,j}^i | j \in \mathcal{F}_t^i)^T$ is the number of packets of each video frame in the STW awaiting transmission at time t . The j th component $b_{t,j}^i$ of \mathbf{b}_t^i denotes the number of packets of frame $j \in \mathcal{F}_t^i$ remaining for transmission at time t . Each packet has size of P bits.

In each time slot t , the i th user takes scheduling action $\mathbf{y}_t^i \triangleq (y_{t,j}^i | j \in \mathcal{F}_t^i)^T$ in the feasible set $\mathcal{P}^i(\mathcal{T}_t^i, \beta_t^i)$, deciding the number of packets to transmit out of \mathbf{b}_t^i . Specifically, the j th component $y_{t,j}^i$ of \mathbf{y}_t^i represents the number of packets of the j th frame within the STW to be transmitted in time slot t . Actions in $\mathcal{P}^i(\mathcal{T}_t^i, \beta_t^i)$ meet the following constraints: (i) every component of \mathbf{y}_t^i obeys $0 \leq y_{t,j}^i \leq b_{t,j}^i$ (*buffer constraint*); (ii) the total number of transmitted packets must satisfy $\|\mathbf{y}_t^i\|_1 = \sum_{j \in \mathcal{F}_t^i} y_{t,j}^i \leq \frac{R \beta_t^i}{P}$, where $\beta_t^i = \beta_t^{i0}$ for direct transmission, i.e., when $z_t^i = 0$, and $\beta_t^i = \beta_t^{i,\text{coop}}$ for cooperative transmission, i.e., when $z_t^i = 1$ (*packet constraint*); (iii) if there exists a frame k that has not been transmitted, and frame j depends on frame k , then $(b_{t,k}^i - y_{t,k}^i) y_{t,j}^i = 0$ so that all packets associated with k are sent before any packet associated with j (*dependency constraint*). The sequence of traffic states $\{\mathcal{T}_t^i : t \in \mathbb{N}\}$ can be modeled as a controllable Markov chain with transition probability function $p(\mathcal{T}_{t+1}^i | \mathcal{T}_t^i, \mathbf{y}_t^i)$ [3].

III. COOPERATIVE PHY LAYER TRANSMISSION

For the direct $i \rightarrow \ell$ QAM link the bit error probability (BEP) $P_t^{i\ell}(h_t^{i\ell}, \beta_t^{i\ell})$ can be upper bounded as

$$P_t^{i\ell}(h_t^{i\ell}, \beta_t^{i\ell}) \leq 4 \exp \left[-\frac{3\gamma |h_t^{i\ell}|^2}{2(2^{\beta_t^{i\ell} T_s} - 1)} \right] \quad (1)$$

where $\gamma \triangleq \frac{\mathcal{E}_s}{N_0}$ is the average SNR per symbol and N_0 is the noise power spectral density. Each direct transmission is subject to a constraint $P_t^{i\ell}(h_t^{i\ell}, \beta_t^{i\ell}) \leq \text{BEP}$ at the PHY layer. Consequently, the achievable data rate $\beta_t^{i\ell}$ is

$$\beta_t^{i\ell} = T_s^{-1} \lceil \log_2(1 + \Gamma |h_t^{i\ell}|^2) \rceil, \Gamma \triangleq \frac{3\gamma}{2} |\log_e(\text{BEP}/4)|^{-1}. \quad (2)$$

We observe that β_t^{i0} is the data rate from user i to the AP. In this case, the number of symbols required to transmit a packet of P bits is equal to $K_t^{i0} \triangleq \lceil P/(\beta_t^{i0} T_s) \rceil$. Thus, the energy required for a direct transmission of one packet is equal to

$$\mathcal{E}_t^{i0} \triangleq K_t^{i0} \mathcal{E}_s = P \mathcal{E}_s / \beta_t^{i0} T_s = P \mathcal{P}_s / \beta_t^{i0} \quad (\text{Joules}) \quad (3)$$

and it is inversely proportional to the achievable data rate β_t^{i0} .

Because of possible error propagation, the end-to-end BEP for a two-hop cooperative transmission is cumbersome to calculate exactly with decode-and-forward relays; therefore,

the relationship that ties $\beta_t^{i,1}, \beta_t^{i,2}$, is not as simple as (2). To simplify the computation of $\beta_t^{i,1}$ and $\beta_t^{i,2}$, we use two different BEP thresholds BEP_1 and $BEP_2 = BEP - BEP_1$ for the first and second hops, respectively. The threshold BEP_1 is typically a large percentage of the total error rate budget, say $BEP_1 = 0.9 BEP$, since the first link is the bottleneck, given that the transmission over the second link can be regarded as a distributed multiple-input single-output system which enjoys cooperative diversity gain. Moreover, we assume that end-to-end error rate is dominated by the frequency of errors over the worst source-to-relay channel, i.e., the link for which $|h_t^{i\ell}|$ is the smallest. Under this assumption, accounting for (2), we can estimate $\beta_t^{i,1}$ in Phase I as

$$\beta_t^{i,1} = T_s^{-1} \left[\log_2 \left(1 + \Gamma_1 \min_{\ell \in \mathcal{C}_t^i} |h_t^{i\ell}|^2 \right) \right] \quad (4)$$

where Γ_1 is obtained from Γ by replacing BEP with BEP_1 . In this phase, which lasts $R \rho_t^i x_t^i$ seconds, the number of symbols sent is $K_t^{i,1} = \lceil P/(\beta_t^{i,1} T_s) \rceil$ and, thus $K_t^{i,1} T_s = P/\beta_t^{i,1} = R \rho_t^i x_t^i$, which leads to $P = R \beta_t^{i,1} \rho_t^i x_t^i$.

Given the set \mathcal{C}_t^i of nodes recruited to serve as relays in Phase II, these nodes, along with the i th user, cooperatively forward the source message by using a randomized STBC rule [11]. More specifically, the decode message is first encoded in a block of QAM symbols $\mathbf{a}_t^i \in \mathbb{C}^{K_t^{i,2}}$ and then mapped onto an *orthogonal* space-time code matrix $\mathcal{G}(\mathbf{a}_t^i) \in \mathbb{C}^{Q \times L}$, where Q is the block length and L denotes the number of antennas in the underlying space-time code. During Phase II, the ℓ th node transmits a linear weighted combination of the columns of $\mathcal{G}(\mathbf{a}_t^i)$, with the weights of the L columns of $\mathcal{G}(\mathbf{a}_t^i)$ contained in the vector $\mathbf{r}_\ell \in \mathbb{C}^L$. We denote with $\mathbf{R} \triangleq (\mathbf{r}_\ell | \ell \in \mathcal{C}_t^i) \in \mathbb{C}^{L \times N_t^i}$ the weight matrix of all the cooperating nodes, where $N_t^i \leq M$ is the cardinality of \mathcal{C}_t^i . Under the randomized STBC rule, the AP observes the space-time coded signal $\mathcal{G}(\mathbf{a}_t^i)$ with *equivalent* channel vector $\tilde{\mathbf{h}}_t^{i,2} \triangleq h_t^{i0} \mathbf{r}_i + \mathbf{R} \mathbf{h}_t^{i,2}$, where $\mathbf{h}_t^{i,2} \triangleq (h_t^{i\ell} | \ell \in \mathcal{C}_t^i)^T \in \mathbb{C}^{N_t^i}$ collects all the channel coefficients between the relay nodes and the AP. Note that the AP only needs to estimate $\tilde{\mathbf{h}}_t^{i,2}$ for coherent decoding and that the randomized coding is decentralized since the ℓ th relay chooses \mathbf{r}_ℓ locally. By capitalizing on the orthogonality of the underlying STBC matrix $\mathcal{G}(\mathbf{a}_t^i)$, the BEP $P_t^{i,2}(\tilde{\mathbf{h}}_t^{i,2}, \beta_t^{i,2})$ over the second hop at the output of the ML detector of the AP using data rate $\beta_t^{i,2}$ (bits/second) can be upper bounded as in (1) by replacing $|h_t^{i\ell}|^2$ and $\beta_t^{i\ell}$ with $\|\tilde{\mathbf{h}}_t^{i,2}\|^2$ and $\beta_t^{i,2}$, respectively. By imposing $P_t^{i,2}(\tilde{\mathbf{h}}_t^{i,2}, \beta_t^{i,2}) \leq BEP_2$, the second hop data rate $\beta_t^{i,2}$ is

$$\beta_t^{i,2} = T_s^{-1} \left[\log_2 [1 + \Gamma_2 (|h_t^{i0}|^2 + \|\mathbf{R} \mathbf{h}_t^{i,2}\|^2)] \right] \quad (5)$$

where Γ_2 is obtained from (2) by replacing BEP with BEP_2 . In this phase, which lasts $R(1 - \rho_t^i) x_t^i$ seconds, the number of symbols needed to transmit a packet of P bits is $K_t^{i,2} = \lceil P/(\beta_t^{i,2} T_s) \rceil$ and, thus, $P/(R_c \beta_t^{i,2}) = R(1 - \rho_t^i) x_t^i$, which leads to $P = R R_c \beta_t^{i,2} (1 - \rho_t^i) x_t^i$, where $R_c \triangleq K_t^{i,2}/Q \leq 1$ is the rate of the orthogonal STBC rule. Consequently, the

total transmission time is given by

$$R x_t^i = P \left(\beta_t^{i,1} + R_c \beta_t^{i,2} \right)^{-1} = P (\beta_t^{i,\text{coop}})^{-1} \quad (6)$$

which reveals the functional dependence of $\beta_t^{i,\text{coop}}$ on $\beta_t^{i,1}$ and $\beta_t^{i,2}$. It is required that $R \beta_t^{i,1} \rho_t^i x_t^i = R R_c \beta_t^{i,2} (1 - \rho_t^i) x_t^i$ and, thus, $\rho_t^i = (1 + \beta_t^{i,1} (\beta_t^{i,2} R_c)^{-1})^{-1}$, which shows that, given the STBC rule, the time fraction ρ_t^i is determined by the data rates in Phase I and II. The cooperative mode is activated only if the cooperative transmission is more data-rate efficient than the direct communication, i.e., only if $\beta_t^{i,\text{coop}} > \beta_t^{i0}$, which from (6) leads to the following condition

$$(\beta_t^{i,1})^{-1} + (R_c \beta_t^{i,2})^{-1} < (\beta_t^{i0})^{-1}. \quad (7)$$

If condition (7) is fulfilled, then the opportunistically optimal cooperation decision is $z_t^i = 1$; otherwise, the i th source transmits to the AP in direct mode and $z_t^i = 0$.

Since cooperation is activated only when $\beta_t^{i,\text{coop}} > \beta_t^{i0}$, node i spends less energy when cooperating. In fact, in the cooperative mode, source i requires

$$\mathcal{E}_t^{i,\text{source}} = \left(K_t^{i,1} + K_t^{i,2} \right) \mathcal{E}_s = P \frac{\mathcal{P}_s}{\beta_t^{i,\text{coop}}} \quad (\text{Joules}) \quad (8)$$

energy per packet. However, the energy spent by each relay

$$\mathcal{E}_t^{i,\text{relay}} = K_t^{i,2} \mathcal{E}_s = P \frac{\mathcal{P}_s}{\beta_t^{i,2} R_c} \quad (\text{Joules}) \quad (9)$$

is inversely proportional to the achievable data rate in Phase II. Therefore, provided that $\beta_t^{i,2} R_c \gg \beta_t^{i0}$, over time, the energy expenditure in relaying another node's data can be compensated in part when nodes exchange the favor. The total energy spent to send $\|\mathbf{y}_t^i\|_1$ packets for user i is

$$\mathcal{E}_t^i(\mathbf{y}_t^i, z_t^i, \mathcal{C}_t^i) = \begin{cases} \|\mathbf{y}_t^i\|_1 \mathcal{E}_t^{i0}, & \text{if } z_t^i = 0; \\ \|\mathbf{y}_t^i\|_1 \left(\mathcal{E}_t^{i,\text{source}} + N_t^i \mathcal{E}_t^{i,\text{relay}} \right), & \text{if } z_t^i = 1. \end{cases} \quad (10)$$

IV. COOPERATIVE MULTI-USER VIDEO TRANSMISSION

Let $\mathbf{s}_t \triangleq (\mathcal{T}_t^1, \mathcal{T}_t^2, \dots, \mathcal{T}_t^M, \mathbf{H}_t) \in \mathcal{S}$ be the global state, where \mathcal{S} is a discrete set of all possible states.³ The sequence of global states $\{\mathbf{s}_t : t \in \mathbb{N}\}$ can be modeled as a controlled Markov process with transition probability function $p(\mathbf{s}_{t+1} | \mathbf{s}_t, \mathbf{y}_t) = p(\mathbf{H}_{t+1}) \prod_{i=1}^M p(\mathcal{T}_{t+1}^i | \mathcal{T}_t^i, \mathbf{y}_t^i)$, where $\mathbf{y}_t \triangleq (\{\mathbf{y}_t^1\}^T, \{\mathbf{y}_t^2\}^T, \dots, \{\mathbf{y}_t^M\}^T)^T$ collects the scheduling actions of all the video users. The immediate utility of the i th user is defined as $u^i(\mathcal{T}_t^i, \mathbf{y}_t^i) \triangleq \sum_{j \in \mathcal{F}_t^i} q_j^i y_{t,j}^i$, which is its experienced total video quality improvement by taking scheduling action \mathbf{y}_t^i under the assumption that quality is incrementally additive [3], [12].

The objective of the MU optimization is the maximization of the *expected discounted sum of utilities* with respect to the joint scheduling action \mathbf{y}_t and the cooperation decision vector $\mathbf{z}_t \triangleq (z_t^1, z_t^2, \dots, z_t^M)^T$ taken in each state \mathbf{s}_t . The

²A specific code is assigned to the source itself. This can be accounted for by simply setting $\mathbf{r}_i = (1, 0, \dots, 0)^T$ and replacing the first row of \mathbf{R} with $(0, \dots, 0)$, whereas the remaining entries of \mathbf{R} are identically and independently generated random variables with zero mean and variance $1/L$.

³To have a discrete set of network states, the individual link states in \mathbf{H}_t are quantized into a finite number of bins.

optimization can be formulated as an MDP that satisfies the following⁴

$$U^*(\mathbf{s}) = \max_{\mathbf{y}, \mathbf{z}} \left\{ \sum_{i=1}^M u^i(\mathcal{T}^i, \mathbf{y}^i) + \alpha \sum_{\mathbf{s}' \in \mathcal{S}} p(\mathbf{H}') \cdot \prod_{i=1}^M p(\mathcal{T}^{i'} | \mathcal{T}^i, \mathbf{y}^i) U^*(\mathbf{s}') \right\}, \forall \mathbf{s} \quad (11)$$

subject to $\mathbf{y}^i \in \mathcal{P}^i(\mathcal{T}^i, \beta^i)$ and $\sum_{i=1}^M x^i \leq 1$, where x^i is the time-fraction allocated to the i th user given its scheduling action \mathbf{y}^i and transmission rate β^i , i.e., $x^i = P(R\beta^i)^{-1} \|\mathbf{y}^i\|_1$, the parameter $\alpha \in [0, 1)$ is the ‘‘discount factor’’, which accounts for the relative importance of the present and future utility, and $\mathcal{P}^i(\mathcal{T}^i, \beta^i)$ is the set of feasible scheduling actions.

Given the distributions $p(\mathbf{H})$ and $p(\mathcal{T}^{i'} | \mathcal{T}^i, \mathbf{y}^i)$ for all i , the above MU-MDP can be solved by the AP using value iteration or policy iteration. However, there are two challenges associated with solving the above MU-MDP. First, the complexity of solving an MDP is proportional to the cardinality of its state-space \mathcal{S} , which, in the above MU-MDP, scales exponentially with the number of users, i.e., M , and with the number of links in \mathbf{H} , i.e., M^2 . We show soon after that the exponential dependence on the number of links in \mathbf{H} can be eliminated. Second, in uplink streaming, the traffic state information is local to the users, so neither the AP nor the users have enough information to solve the above MU-MDP. In what follows, relying on [3], we show that the considered optimization can be approximated to make it amenable to a distributed solution.

If we can show that the optimal opportunistic (i.e., myopic) cooperation decision is also long-term optimal, then the detailed network state information does not need to be included in the MU-MDP. The following theorem shows that the optimal opportunistic cooperation decision, which maximizes the immediate transmission rate, is also long-term optimal.

Theorem 1 (Opportunistic cooperation is optimal): If cooperation incurs zero cost to the source and relays, then the optimal opportunistic cooperation decision, which maximizes the immediate throughput, is also long-term optimal.

Proof: The proof can be found in [13]. ■

To intuitively understand why maximizing the immediate transmission rate at the PHY layer is long-term optimal, consider what happens when a user chooses not to maximize its immediate transmission rate. Two things can happen: either less packets are transmitted overall because of packet expirations; or, the same number of packets are transmitted overall, but their transmission incurs additional resource costs since transmitting the same number of packets at a lower rate requires more resources. In either case, the long-term utility is suboptimal. A consequence of Theorem 1 is that the cooperation decision vector \mathbf{z} does not need to be included in the MU-MDP. Instead, it can be determined opportunistically by selecting \mathbf{z} to maximize the immediate transmission rate. This means that the MU-MDP does not need to include the high-dimensional network state.

⁴In this section, since we model the problem as a stationary MDP, we omit the time index when it does not create confusion. In place of the time index, we use the notation $(\cdot)'$ to denote a state variable in the next time step.

Although the users’ MDPs do not need to include the high-dimensional network state, the optimal resource allocation and scheduling strategies still depend on it; however, instead of tracking \mathbf{H}_t , it is sufficient to track the users’ optimal opportunistic transmission rates provided by the PHY layer, i.e., β_t^i for all i . Under the assumption that the channel coefficients are i.i.d. random variables with respect to t , β_t^i can also be modeled as an i.i.d. random variable with respect to t . We let $p(\beta^i)$ denote the probability mass function (pmf) from which β_t^i is drawn. We note that $p(\beta^i)$ depends on $p(\mathbf{H})$ and the deployed PHY layer cooperation algorithm. Based on the above, we can simplify the maximization problem in (11). Let us define the i th user’s state as $s^i \triangleq (\mathcal{T}^i, \beta^i) \in \mathcal{S}^i$ and redefine the global state as $\mathbf{s} \triangleq (s^1, \dots, s^M)^T$. In Section V, we describe how β^i is determined, but for now we will take for granted that it is known. Because the optimization does not need to include the cooperation decision, the maximization of the expected sum of discounted utilities in (11) can be simplified by only maximizing with respect to the scheduling action \mathbf{y} in each state \mathbf{s} , that is,

$$U^*(\mathbf{s}) = \max_{\mathbf{y}} \left\{ \sum_{i=1}^M u^i(\mathcal{T}^i, \mathbf{y}^i) + \alpha \sum_{\mathbf{s}' \in \mathcal{S}} \cdot \prod_{i=1}^M p(s^{i'} | s^i, \mathbf{y}^i) U^*(\mathbf{s}') \right\}, \forall \mathbf{s} \quad (12)$$

subject to $\mathbf{y}^i \in \mathcal{P}^i(\mathcal{T}^i, \beta^i)$, $\sum_{i=1}^M x^i \leq 1$, where $p(s^{i'} | s^i, \mathbf{y}^i) = p(\beta^{i'}) p(\mathcal{T}^{i'} | \mathcal{T}^i, \mathbf{y}^i)$.

As in [3], eq. (12) can be reformulated as an unconstrained MDP using Lagrangian relaxation. By imposing a uniform resource price λ , which is independent of the multi-user state, the resulting MU-MDP can be decomposed into M MDPs, one for each user. These local MDPs obey (see [3])

$$U^{i,*}(s^i, \lambda) = \max_{\mathbf{y}^i} \left[u^i(\mathcal{T}^i, \mathbf{y}^i) - \lambda \left(x^i - \frac{1}{M} \right) + \alpha \sum_{s^{i'} \in \mathcal{S}} p(s^{i'} | s^i, \mathbf{y}^i) U^{i,*}(s^{i'}, \lambda) \right] \quad (13)$$

where $\hat{U}^*(\mathbf{s}) = \min_{\lambda \geq 0} \sum_{i=1}^M U^{i,*}(s^i, \lambda) \approx U^*(\mathbf{s})$, subject to $\mathbf{y}^i \in \mathcal{P}^i(\mathcal{T}^i, \beta^i)$. Importantly, the i th user’s dynamic programming equation defines the optimal scheduling action as a function of the i th user’s state, rather than the global state \mathbf{s} . Herein, the i th user solves (13) offline using value iteration; however, it can be easily solved online using reinforcement learning as in [3] and [14]. Also, note that due to the distributed nature of the proposed algorithm, the stage resource constraint $\sum_{i=1}^M x_t^i \leq 1$ is not guaranteed to be satisfied during convergence or at steady-state. Because the stage resource constraint may be violated, it must be enforced separately by the AP, which we assume normalizes the requested resource allocations and, subsequently, has the users recompute their scheduling policies to satisfy the new allocations.

Although the optimization can be decomposed across the users, the optimal resource price λ still depends on all of the users’ resource demands. Hence, λ must be determined by the AP. The resource price can be numerically computed by the AP using the subgradient method. Because the focus of this

TABLE I

THE PROPOSED PROTOCOL FOR RANDOMIZED STBC COOPERATION.

Step 1) The i th source initiates the handshaking by transmitting the RTS frame, which announces its desire to transmit data and also includes training symbols that are used by the other nodes for channel estimation.
Step 2) From the RTS message, the AP estimates the channel coefficients h_t^{i0} and, hence, determines β_t^{i0} . At the same time, by passively listening to all the RTS messages occurring in the network, the other nodes estimate their respective channel parameters $h_t^{i\ell}$, for $\ell \in \{1, 2, \dots, M\} - \{i\}$, and, thus, determine $\beta_t^{i\ell}$.
Step 3) The AP responds with the CRS message that provides feedback on β_t^{i0} to all the candidate cooperative nodes and the source, as well as a second parameter $0 < \xi_t < 1$, which is used to recruit relays.
Step 4) From the CRS message, the i th source learns that a cooperative transmission may take place and, if such a communication mode will be confirmed by the AP, the data rate to be used in Phase I is $\beta_t^{i,1} = \frac{\beta_t^{i0}}{\xi_t}$.
Step 5) After receiving the CRS frame, the candidate cooperative nodes can self-select themselves according to the rule

$$C_t^i = \left\{ \ell : \frac{\beta_t^{i0}}{\beta_t^{i\ell}} \leq \xi_t \right\} \quad (14)$$

where $\beta_t^{i\ell}$ is defined using (2) by replacing BEP with BEP_1 . The nodes belonging to the formed group C_t^i send in unison the HTS message using randomized STBC of size L as described in Section III, which piggybacks training symbols that are used by the AP to estimate the cooperative channel vector $\mathbf{R}\mathbf{h}_t^{i,2}$.

Step 6) After estimating the channel of the cooperative link, the AP computes the data rate $\beta_t^{i,2}$ by resorting to (5) and verifies the fulfillment of the following condition $\frac{1}{R_c \beta_t^{i,2}} < \frac{1-\xi_t}{\beta_t^{i0}}$. If such a condition holds, then, it can be inferred that cooperation is better than direct transmission, i.e., condition (7) is satisfied: in this case, $z_t^i = 1$. Otherwise, cooperation is useless: in this case, $z_t^i = 0$. Therefore, the AP responds with a CTS frame, which conveys the following information: (i) the cooperation decision z_t^i ; (ii) if $z_t^i = 1$, the data rate $\beta_t^{i,2}$ in Phase II given by (5); (iii) the resource price λ (see Section IV).
Step 7) If $z_t^i = 1$ in the CTS frame, the source proceeds with sending in Phase I its data frame at data rate $\beta_t^{i,1}$; otherwise, if $z_t^i = 0$, it transmits in direct mode at the data rate β_t^{i0} .

Step 8) If $z_t^i = 1$ in the CTS frame, along with the source, the self-recruited relays cooperatively transmit in Phase II the data frame at rate $\beta_t^{i,2}$; otherwise, if $z_t^i = 0$, they remain silent.

Step 9) The AP finishes the procedure by sending back to the source an acknowledgement (ACK) message.

multiple access with collision avoidance (CSMA/CA), which is extended to include a helper-ready to send (HTS) control message that is cooperatively transmitted by the relays using randomized STBC and a cooperative recruitment signal (CRS) that is sent by the AP to recruit relays. The idea of sending the HTS frame in cooperative mode has been originally proposed in [16], albeit for an entirely different recruitment policy.

All the control frames are transmitted at the base rate β_0 such that they can be decoded correctly, and the thresholds BEP_1 and BEP_2 , as well as L and R_c , are fixed parameters that are known at all the nodes. The protocol requires the steps detailed in Table I. We would like to highlight that, similar to the data transmitted in Phase II, the HTS message is a cooperative signal, i.e., all relays jointly deliver the HTS frame using randomized STBC at the same time and, hence, simultaneous transmissions do not cause a collision. From Table I, a key observation is that the selection of the set C_t^i using (14) is done in a distributed way since, having access to the channel state from the source i to itself, i.e., $h_t^{i\ell}$, the ℓ th candidate cooperative node can *autonomously* determine if, by cooperating, it can improve the data rate of node i . We also note that only four control messages for each source are exchanged, independent of the number of recruited relays, thanks to the cooperative randomized coding of the HTS frames. A caveat is that the two parameters ξ_t and L need to be chosen, in principle, based on global network information. A learning framework would be very appropriate for their selection but we defer the treatment of this aspect to future work. Finally, as for the impact of L on the network performance, randomized codes have been shown to behave statistically like their non-randomized counterparts [11], with deep-fade events that are as frequent as those of L independent channels, as long as $N_t^i \geq L + 1$.

VI. NUMERICAL RESULTS

We consider a network with 50 potential relay nodes placed randomly and uniformly throughout the 100 m coverage range of a single AP. We specify the placement of the video source(s) separately for each experiment. Let $\eta_t^{i\ell}$ denote the distance in meters between the i th and ℓ th nodes. The fading coefficient $h_t^{i\ell}$ over the $i \rightarrow \ell$ link is modeled as an i.i.d. $\mathcal{CN}(0, (\eta_t^{i\ell})^{-2})$ random variable. Additionally, we assume that the entries of \mathbf{R} , defined in Section III, are i.i.d. $\mathcal{CN}(0, \frac{1}{L})$ random variables, where L is the length of the STBC. If an error occurs in the packet transmission, then the packet remains in the frame buffer to be retransmitted in a future time slot (assuming the packet's deadline has not passed). We consider three scenarios: (i) a single source node is placed between 10 m and 100 m directly to the right of the AP (*single source*); (ii) three homogeneous video sources, which are placed 20 m, 45 m, and 80 m from the AP at angles 25° , -30° , and 0° , respectively, stream the Foreman sequence (CIF resolution, 30 Hz framerate, encoded at 1.5 Mb/s) to the AP (*homogeneous video sources*); (iii) three video sources, which are located as in the previous scenario, transmit heterogeneous video content to the AP (*heterogeneous video sources*), i.e., video user 1 streams the Coastguard sequence (CIF, 30 Hz, 1.5 Mb/s), video user 2 streams the Mobile sequence (CIF, 30 Hz, 2.0 Mb/s), and video user 3 streams the Foreman sequence (CIF,

paper is on the interaction between the MU video transmission and the cooperative PHY layer, we refer the interested reader to [3] for complete details on the dual decomposition outlined in this subsection and the subgradient update.

V. RECRUITMENT PROTOCOL

Herein, we define our opportunistic strategy to select distributively the set of relays C_t^i and decide z_t^i at the AP.

Note that the AP can exactly evaluate $\beta_t^{i,2}$ in (5) because it can estimate h_t^{i0} and $\mathbf{R}\mathbf{h}_t^{i,2}$ via training as mentioned in Section III. However, the trouble in recruiting relays on-the-fly is that the AP and the relays cannot directly compute $\beta_t^{i,1}$ given by (4), since they cannot estimate the channel coefficients $h_t^{i\ell}$, for all $\ell \in C_t^i$. Some MAC randomized protocols have recently been proposed [15], [16], which get around the problem that the AP and the relays do not have the necessary channel state information to determine $\beta_t^{i,1}$. We propose a much simpler recruitment scheme that is based on the closed-form formulas (4) and (5). The proposed four-way protocol is reminiscent of the request-to-send (RTS) and clear-to-send (CTS) handshaking used in carrier sense

TABLE II
SIMULATION PARAMETERS.

Parameter	Description	Value
L	Length of the STBC	2
R_c	Rate of orthogonal STBC rule	1
ξ	Self-selection parameter	0.1, 0.2, 0.3, 0.4, 0.5
P	Packet size	8000 bits
BEP	Bit error probability target (uncoded)	10^{-3}
δ	Path loss exponent	3
R_{cell}	WLAN coverage radius (5 dB SNR at boundary)	100 m
M	Number of nodes (excluding the AP)	50
α	Discount factor	0.80
$1/T_s$	Symbol rate (symbols per second)	625000 or 1250000
\mathcal{E}_s	Symbol energy (normalized)	$\frac{T_s}{P}$ Joules

30 Hz, 1.5 Mb/s). The proposed framework can be applied using any video coder to compress the video data. However, for illustration, we use a scalable video coding scheme [17], which is attractive for wireless streaming applications because it provides on-the-fly application adaptation to channel conditions, support for a variety of wireless receivers with different resource and power constraints, and easy prioritization of video packets. The relevant simulation parameters are given in Table II, where, in the homogeneous and heterogeneous scenarios, we simulate a network with a “high” transmission rate, using the symbol rate $\frac{1}{T_s} = 1250000$, and a network with a “low” transmission rate, using the symbol rate $\frac{1}{T_s} = 625000$ symbols/second.

A. Transmission rates and energy consumption

In this subsection, we consider the single source scenario described above. Fig. 1 illustrates the performance of the proposed cooperation protocol for time-invariant self-selection parameter values $\xi_t = \xi \in \{0.1, 0.2, \dots, 0.5\}$, and the performance of direct transmission, given a single source transmitting to the AP. Note that these results hold regardless of the symbol rate. In particular, the “transmission rate” in Fig. 1(a) is presented in terms of the spectral efficiency (bits/second/Hz); the probability of cooperation in Fig. 1(b) and the average number of recruited relays in Fig. 1(c) only depend on the spectral efficiency; and the energy results reported in Figs. 1(d-f) are normalized by setting $\mathcal{E}_s = \frac{T_s}{P}$ (or, equivalently, $\mathcal{P}_s = \frac{1}{P}$) in (3), (8), and (9).

From Fig. 1(a), it is clear that nodes further from the AP utilize cooperation more frequently than nodes closer to the AP. This is because, on average, distant nodes have the feeblest direct signals to the AP due to path-loss and, therefore, have the most to gain from the channel diversity afforded to them by cooperation. It is also clear from Fig. 1(a) that cooperation is utilized more frequently as the self-selection parameter ξ increases. This is because, as illustrated in Fig. 1(c), more relays satisfy the self-selection condition in step 5 of Table I

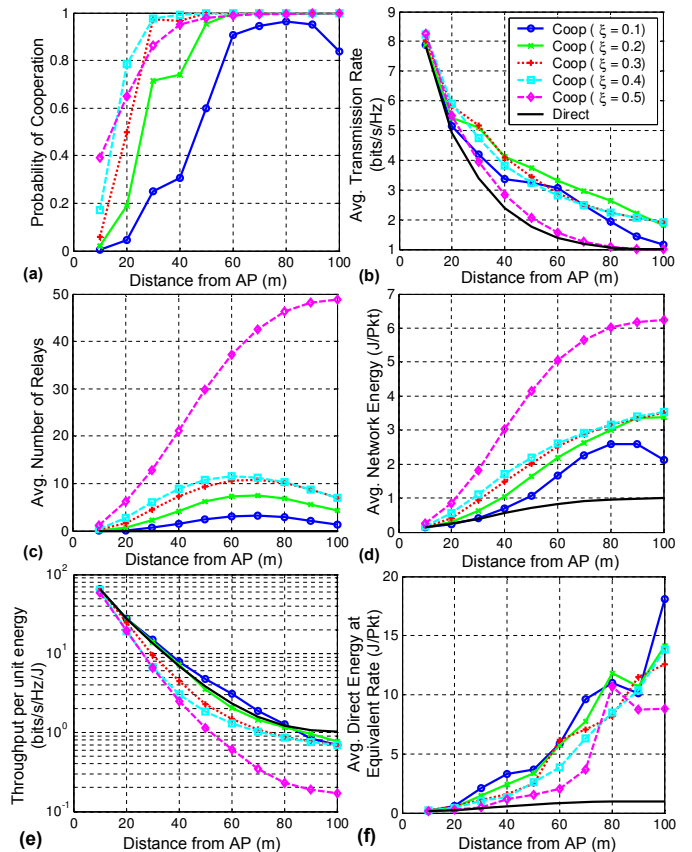


Fig. 1. Cooperative transmission statistics. (a) Average transmission rate. (b) Probability of cooperation being optimal. (c) Average number of recruited relays. (d) Average energy consumed in the network per packet transmission. (e) Throughput per unit energy. (f) Average energy required by the source to transmit one packet at the rate $\beta_t^{i0} = \beta_t^{i,\text{coop}}$.

for larger values of ξ . However, larger values of ξ yield relay nodes for which $\frac{\beta_t^{i0}}{\beta_t^{i\xi}}$ is large, which leads to a bad transmission rate over the bottleneck hop-1 cooperative link. Due to this poor bottleneck rate and the large number of recruited relays, the average transmission rate shown in Fig. 1(b) declines for $\xi > 0.2$ even while the total energy consumption increases as illustrated in Fig. 1(d). In contrast, lower values of the self-selection parameter (e.g. $\xi < 0.2$) lead to too few nodes being recruited to achieve large cooperative gains, but yield lower energy consumption. Interestingly, the same properties of relay nodes that are desirable for achieving the best transmission rate – a balance between the number and quality of relays – is also important for achieving a high throughput-to-energy ratio. For example, Fig. 1(e) shows us that at 100 m from the AP, the average throughput-to-energy ratio for cooperative transmission with $\xi = 0.2$ is a little less than 0.8, which is close to the throughput-to-energy ratio of a direct transmission, which is 1 at 100 m.

Although the average network energy required to support a cooperative transmission is larger than that required for a direct transmission, this increase is moderate compared to the amount of energy the source node would have to expend in order to achieve the same transmission rate as the cooperative transmission, i.e., to attain $\beta_t^{i0} = \beta_t^{i,\text{coop}}$ requires a large increase in the transmission power with respect to the cooperative case. This is illustrated in Fig. 1(f), where, for

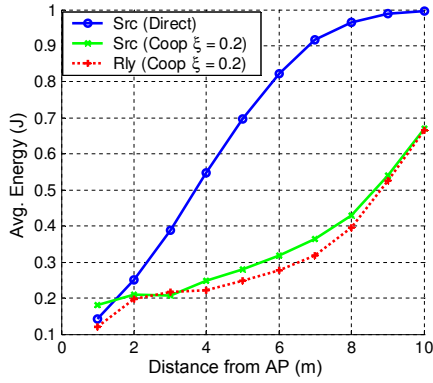


Fig. 2. Average energy consumed by source (Src) during direct and cooperative transmission, and average energy consumed by a relay (Rly) during cooperative transmission.

example, at 100 m it is shown that transmitting in the direct mode at the rate attainable under cooperative transmission with $\xi = 0.2$ requires approximately 13.5 normalized Joules/Packet compared to approximately 3.5 normalized Joules/Packet in the cooperative case shown in Fig. 1(d).⁵

In the sequel, we let the self-selection parameter $\xi_t = \xi = 0.2$ because, as illustrated in Figs. 1(b,e), this value provides a large average transmission rate over the AP's entire coverage range and a high throughput-to-energy ratio. With $\xi = 0.2$, Fig. 2 illustrates the average energy consumed by the source and relay nodes. Under a cooperative transmission, the source node actually uses less power than under a direct transmission, which partially compensates for the extra energy it may expend acting as a relay for other nodes.

B. Transmission rate, resource price, and resource utilization

Fig. 3 illustrates the average transmission rates achieved by the video users in the homogeneous and heterogeneous scenarios in networks that support high and low transmission rates. Recall that the resource cost x_t^i incurred by user i is inversely proportional to the transmission rate, which decreases as the distance to the AP increases due to path loss. Hence, when only direct transmission is available, user 3 tends to resign itself to a low average transmission rate because the cost of using resources is too high. Cooperation increases the average transmission rate, thereby providing user 3 lower cost access to the channel to transmit more data.

In the homogeneous scenario illustrated in Fig. 3(a), cooperation tends to equalize the resource allocations to the three users (this is especially evident in the cooperative case with a high transmission rate). This is because the homogeneous users have identical utility functions; thus, when sufficient resources are available, it is optimal for them to all operate at the same point of their resource-utility curves. In contrast, when heterogeneous users with different utility functions are introduced, the transmission rates change to reflect the priorities of the different users' video data, with

⁵The results in Fig. 1(f) were obtained by fixing the transmission rate and adapting the symbol energy, which is in contrast to the current problem formulation in which we fix the symbol energy and adapt the transmission rate. Specifically, we calculated the symbol energy $\tilde{\mathcal{E}}_s$ required to set $\beta_t^{i\ell} = \beta_t^{i,\text{coop}}$ by rearranging (2). Note that we could also force $\beta_t^{i,\text{coop}} = \beta_t^{i0}$ to achieve lower energy consumption at the same transmission rate as the direct mode.

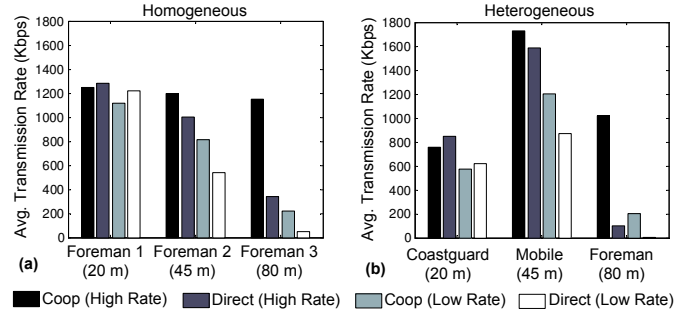


Fig. 3. Average transmission rates. (a) Homogeneous video sources. (b) Heterogeneous video sources.

TABLE III
RESOURCE PRICES AND RESOURCE UTILIZATION.

Streaming Scenario	Transmission Mode	Resource Price (High / Low)	Utilization (High / Low)
Homogeneous	Direct	45.79 / 42.97	0.73 / 0.67
	Cooperative	38.72 / 52.56	0.88 / 0.75
	Change	-6.93 / 9.59	0.15 / 0.08
Heterogeneous	Direct	51.01 / 53.17	0.66 / 0.68
	Cooperative	48.02 / 71.94	0.89 / 0.77
	Change	-2.99 / 18.77	0.23 / 0.09

more resources going to the highest priority video user (user 2 in our simulations).

Recall that users autonomously optimize their resource allocation and scheduling actions given the resource price λ announced by the AP. Table III illustrates the optimal resource prices in the homogeneous and heterogeneous scenarios along with the average network resource utilization, i.e. the average of $\sum_{i=1}^M x_t^i$. There are several interesting results in Table III. First, the average network resource utilization is often considerably less than the total available resources. This is due to the distributed nature of the resource allocation and scheduling algorithm, which requires users to be conservative in their resource usage to ensure feasible allocations. Second, in the cooperative transmission mode, the resource price tends to increase and the utilization tends to decrease when going from a high rate to a low rate network, regardless of the streaming scenario. The resource price increases because the network supports lower rates, but the demand stays the same. The utilization decreases because lower rates yield a coarser set of feasible resource allocations for each user. Third, in the high rate network, the resource price tends to decrease and the utilization tends to increase when going from the direct to the cooperative transmission mode, regardless of the streaming scenario. The resource price decreases because cooperation floods the network with resources without significantly impacting demand. The utilization increases because the cooperative transmission mode supports higher transmission rates, which yield a finer set of feasible resource allocations for each user. Finally, in the low rate network, the resource price and utilization tend to increase when going from the direct to the cooperative transmission mode. In contrast to the high rate network, the resource price *increases* because users that resigned themselves to very low transmission rates in the direct scenario suddenly demand resources when cooperation is enabled. The resource price increases in our simulations

TABLE IV
AVERAGE VIDEO QUALITY (PSNR).

Streaming Scenario	Transmission Mode	Video User 1 @ 20 m (High / Low)	Video User 2 @ 45 m (High / Low)	Video User 3 @ 80 m (High / Low)
Homogeneous		Foreman	Foreman	Foreman
	Direct	36.82 dB / 36.51 dB	35.85 dB / 30.20 dB	29.89 dB / --- dB
	Cooperative	36.69 dB / 35.82 dB	36.58 dB / 34.83 dB	36.04 dB / 27.12 dB
	Change	-0.13 dB / -0.69 dB	0.73 dB / 4.63 dB	6.15 dB / --- dB
Heterogeneous		Coastguard	Mobile	Foreman
	Direct	32.30 dB / 31.09 dB	26.74 dB / 24.53 dB	25.94 dB / --- dB
	Cooperative	31.94 dB / 30.89 dB	27.14 dB / 25.8 dB	35.69 dB / 27.12 dB
	Change	-0.36 dB / -0.20 dB	0.4 dB / 1.27 dB	9.75 dB / --- dB

because users that would like to transmit video, but are too far from the AP for a direct transmission, are essentially absent from the network when only direct transmission is available, and therefore do not significantly impact the resource price and resource utilization; however, when cooperation is enabled, these users are suddenly within range of the AP, and will therefore demand resources, which increases congestion. As in the other cases, the utilization increases because the transmission rate increases.

C. Video quality comparison

Table IV compares the video quality in terms of the peak-signal-to-noise ratio (PSNR in dB) of the luminance channel obtained in the homogeneous and heterogeneous scenarios. In the network that supports a high transmission rate, the user furthest from the AP (user 3) benefits on the order of 5-10 dB PSNR from cooperation, while the video user closest to the AP (user 1) is penalized by less than 0.4 dB PSNR. In the network that only supports low transmission rates, user 3 goes from transmitting too little data to decode the video (denoted by “---”) to transmitting enough data to decode at low quality, while penalizing user 1 by less than 0.8 dB PSNR.

VII. CONCLUSION

We introduced a cooperative multiple access strategy that enables nodes with high priority video data to be serviced while simultaneously exploiting the diversity of channel fading states in the network. We analytically proved that opportunistic (myopic) cooperation strategies are optimal, and therefore the users’ only need to know their experienced cooperative transmission rates to determine their optimal resource allocation and scheduling policies. We also proposed a randomized STBC cooperation protocol that enables nodes to opportunistically and distributively self-select themselves as cooperative relays. The proposed cooperation strategy significantly improves the video quality of nodes with feeble direct links to the AP, without significantly penalizing other users, and with only moderate increases in total network energy consumption.

REFERENCES

- [1] E. Maani, P. Pahalawatta, R. Berry, T.N. Pappas, and A.K. Katsaggelos, “Resource Allocation for Downlink Multiuser Video Transmission over Wireless Lossy Networks,” *IEEE Trans. Image Process.*, vol. 17, issue 9, pp. 1663-1671, Sept. 2008.
- [2] G-M. Su, Z. Han, M. Wu, and K.J.R. Liu, “Joint Uplink and Downlink Optimization for Real-Time Multiuser Video Streaming Over WLANs,” *IEEE J. Sel. Areas Commun.*, vol. 1, no. 2, pp. 280-294, Aug. 2007.
- [3] F. Fu and M. van der Schaar, “A Systematic Framework for Dynamically Optimizing Multi-User Video Transmission,” *IEEE J. Sel. Areas Commun.*, vol. 28, pp. 308-320, Apr. 2010.
- [4] R. Knopp and P. A. Humblet, “Information capacity and power control in single-cell multiuser communications,” *Proc. IEEE ICC*, vol. 1, pp. 331-335, June 1995.
- [5] P. Viswanath, D. N. C. Tse, R. Laroia, “Opportunistic beamforming using dumb antennas,” *IEEE Trans. Inf. Theory*, vol. 48, no. 6, pp. 1277-1294, June 2002.
- [6] J.N. Laneman and G.W. Wornell, “Distributed space-time block coded protocols for exploiting cooperative diversity in wireless networks,” *IEEE Trans. Inf. Theory*, vol. 49, no. 10, pp. 2415-2425, Oct. 2003.
- [7] A. Sendonaris, E. Erkip, and B. Aazhang, “User cooperation diversity – Part I & II,” *IEEE Trans. Commun.*, vol. 51, no. 11, pp. 1927-1948, Nov. 2003.
- [8] J.N. Laneman, D. Tse, and G.W. Wornell, “Cooperative diversity in wireless networks: efficient protocols and outage behavior,” *IEEE Trans. Inf. Theory*, vol. 50, no. 12, pp. 3062-3080, Sept. 2004.
- [9] T. C.-Y. Ng and W. Yu, “Joint optimization of relay strategies and resource allocations in cooperative cellular networks,” *IEEE J. Sel. Areas Commun.*, vol. 25, no. 2, pp. 328-339, Feb. 2007.
- [10] O. Alay, P. Liu, Z. Guo, L. Wang, Y. Wang, E. Erkip, and S. Panwar, “Cooperative layered video multicast using randomized distributed space time codes”, in *Proc. IEEE INFOCOM Workshop*, pp. 1-6, Apr. 2009.
- [11] B. Sirkeci-Mergen and A. Scaglione, “Randomized space-time coding for distributed cooperative communication”, *IEEE Trans. Signal Process.*, vol. 55, pp. 5003-5017, Oct. 2007.
- [12] P. Chou and Z. Miao, “Rate-distortion optimized streaming of packetized media”, *IEEE Trans. Multimedia*, vol. 8, no. 2, pp. 390-404, Apr. 2006.
- [13] N. Mastronarde, F. Verde, D. Darsena, A. Scaglione, and M. van der Schaar, “Transmitting important bits and sailing high radio waves: a decentralized cross-layer approach to cooperative video transmission,” Technical Report. Available online: <http://arxiv.org/abs/1102.5437>
- [14] N. Salodkar, A. Karandikar, V. S. Borkar, “A stable online algorithm for energy-efficient multiuser scheduling,” *IEEE Trans. Mobile Comput.*, vol. 9, no. 10, pp. 1391-1406, Oct. 2010.
- [15] F. Verde, T. Korakis, E. Erkip, and A. Scaglione, “A simple recruitment scheme of multiple nodes for cooperative MAC,” *IEEE Trans. Commun.*, vol. 58, no. 9, pp. 2667-2682, Sept. 2010.
- [16] P. Liu, C. Nie, T. Korakis, E. Erkip, S. Panwar, F. Verde, and A. Scaglione, “STiMAC: A MAC Protocol for Robust Space-Time Coding in Cooperative Wireless LANs.” Available online: <http://arxiv.org/abs/1105.3977v2>.
- [17] J.R. Ohm, “Three-dimensional subband coding with motion compensation”, *IEEE Trans. Image Process.*, vol. 3, no. 5, pp. 559-571, Sept. 1994.

Nicholas Mastronarde (M’11) is an Assistant Professor in the Department of Electrical Engineering at the State University of New York (SUNY) at Buffalo (see <http://www.sens.buffalo.edu/~nmastron> for further information).

Francesco Verde (M’10) is an Assistant Professor of Signal Theory with the Department of Biomedical, Electronic and Telecommunication Engineering, University of Napoli Federico II. Since 2010, he has served as Associate Editor for the IEEE Transactions on Signal Processing (see <http://www.die.unina.it/francesco.verde/> for further information).

Donatella Darsena (M’06) is an Assistant Professor with the Department for Technologies, University of Napoli Parthenope, Italy (see <http://www.dit.uniparthenope.it> for further information).

Anna Scaglione (SM’09-F’11) is Professor in Electrical Engineering at the University of California at Davis, CA. Prior to this she was postdoctoral researcher at the University of Minnesota in 1999-2000, Assistant Professor at the University of New Mexico in 2000-2001, Assistant and Associate Professor at Cornell University in 2001-2006 and 2006-2008, respectively (see <http://www.ece.ucdavis.edu/scaglione/for> for further information).

Mihaela van der Schaar (F’10) is Chancellor’s Professor of Electrical Engineering at University of California, Los Angeles. She is an IEEE Fellow, a Distinguished Lecturer of the Communications Society for 2011-2012, the Editor in Chief of IEEE Transactions on Multimedia and a member of the Editorial Board of the IEEE Journal on Selected Topics in Signal Processing (see <http://medianetlab.ee.ucla.edu/> for further information).